Measurements of the Electromagnetic Emissions from the MUSES-C Ion Engine System*†

Kazutaka Nishiyama, Yukio Shimizu, Ikkoh Funaki, Hitoshi Kuninaka, Kyoichiro Toki
Institute of Space and Astronautical Science
3-1-1 Yoshinodai
Sagamihara, Kanagawa, Japan 2298510
+81-42-759-8288
nishiyama@ep.isas.ac.jp

IEPC-01-112

Radiated electric field emissions from the prototype model of the Ion Engine System (IES) of the MUSES-C mission were measured in accordance to MIL-STD-461E. The average noise level exceeded the narrowband specification at frequencies less than 5 MHz. The microwave discharge neutralizer generates a broadband noise and narrowband oscillations which have a fundamental frequency of about 160 kHz and are accompanied by its harmonics up to the 5th. The leakage of the 4.25 GHz microwave for plasma production and its second harmonic were 65 dB and 35 dB above specification, respectively. The X-band receiver onboard the MUSES-C measured the noise from the IES at the up-link frequency of 7.16 GHz through a horn antenna. This susceptibility test proved that the microwave discharge ion thruster will never interfere the deep space microwave communication.

Introduction

In satellites driven by electric propulsion, considerable amount of electric power generated in space is put into discharge plasma. There are many cases in which exposing the current path to the space is inevitable, and this will become large electromagnetic noise source. There is a review by Sovey et al. [1] on the results of ground-based and flight tests on Electromagnetic Interference (EMI) in electric propulsion systems which dates back to the 1980's. As for ion propulsion systems developed after the SERT-I project, which is considered to be the first ion thruster flight, all of them including the Japanese ETS-III [2],[3], ETS-VI [4], German RIT-10 [5] and British T5 [6] have undergone ground-based EMI tests. Although it is usual practice to follow the U.S. military standard MIL-STD-461 for EMI documentation of components onboard satellites, such requirements have not been fully satisfied by any electric propulsion systems (whether they be ion thrusters or other type) developed up until now. In the case of NASA's NSTAR ion engine used by the DS1 probe, which is presently operating in interplanetary space, an EMI measuring device (Plasma Wave Detector) is onboard as one of several environment measuring devices [7].

An ion engine system (IES) for the MUSES-C asteroid sample return mission is now under development at the Institute of Space and Astronautical Science (ISAS), Japan[8]. The spacecraft will be launched in the winter of 2002 on an ISAS' M-V rocket from the Kagoshima Space Center located on the southern tip of the Japanese island of Kyushu. MUSES-C's EMI specifications applied to all onboard components are a modification of the radiated emission (RE02) specification of MIL-STD-461C. The MUSES-C/IES will be the first ion propulsion system using microwave discharges, and its electromagnetic compatibility (EMC) with spacecraft has not been confirmed until now. Though it was estimated that the microwave of 4.25 GHz generated by traveling wave tube amplifiers could leak to some extent, what sort of electromagnetic noise is radiated and from where exactly, were questions that remained to be answered. Accordingly, we planed two RE02 measurements: one involving both an ion engine and neutralizer and another one for just the neutralizer.

The degradation of the sensitivity of the X-band receiver (XRX) is caused when the radiated emission from IES is larger than the thermal noise level in the uplink frequency of the MUSES-C's XRX. In the RE specification of the MUSES-C deep space probe,

* Presented as Paper IEPC-01-112 at the 27th International Electric Propulsion Conference, Pasadena, CA, 15-19 October, 2001.
† Copyright © 2001 by Kazutaka Nishiyama. Published by the Electric Rocket Propulsion Society with permission.

spurious radiations in the frequency range of ± 5 MHz with centers of 7.16 GHz and 6.36 GHz is limited to -6, +34 dBμV/m, respectively. The former is for the XRX signal band and the latter is for its image band. Since it is difficult to measure such weak noise with standard EMI test equipments, a compatibility test using the IES and the XRX was necessary in order to assure that the IES satisfied the requirements. Hence, an interference check which used a RF/IF signal processing part of the XRX as a high-gain amplifier was carried out after the IES's EMI test. There is a general concern about the attenuation and phase change of the communication wave propagating through the plasma plume. Although this is also one type of EMC problem between the electric propulsion and the communication systems of the satellite, we consider this not be the case for MUSES-C, in which thruster plume density is too low to degrade the communication link, according to the result of experiment and analysis [9].

In addition to radiated emissions, Conducted Emissions (CE) from the IES power processing unit (IPPU), for the ion beam acceleration with a power consumption of 1.2 kW and with three thruster units operating via the spacecraft power bus line, were also investigated. Also, the CE-02 measurement of the noise in the power line current was envisaged using a prototype model (PM) of the IPPU and a commercial power supply as an unstabilized power bus simulator. Measurements of conducted noise on the screen grid line and neutralizer line from IPPU were also carried out in order to examine correlation with the conducted noise on the bus line, as well as the noise source.

Experimental Arrangement

In this paper three EMI test results summarized in Table 1 will be reported. Antenna configurations and the bandwidth of a spectrum analyzer in all experiments are according to specifications in the latest edition of MIL-STD-461E. In the RE02 measurements, several types of antennas, which were selected depending on the frequency range, a preamplifier, a preselector and a spectrum analyzer were utilized. These antennas include an active monopole, a biconical one, and two conical log spiral antennas of different sizes depending on the frequency range. Horn antennas, spectrum analyzers, a digital voltmeter were employed in the interference test with the XRX.

Table 1. Summary of MUSES-C/IES EMI Tests.

	IES RE02 & X-band receiver interference	Neutralizer RE02	IES CE02
Environment	Anechoic chamber	EMI chamber	IES endurance test room
Chamber	Upright cylindrical glass chamber	T-shaped glass chamber	Metal chamber
Pumping system	1 cryogenic pump	1 oil diffusion pump and 1 rotary pump	8 cryogenic pumps
Ion source	PM	-	PM
Neutralizer	PM	PM	PM
PPU	GSE	GSE	GSE / IPPU (PM)
Microwave generator	FM	GSE	GSE
Propellant feed system	GSE	GSE	GSE
Thruster controller	ITCU (PM)	Personal computer	Workstation
Frequency	14 kHz ~ 10 GHz, 7.16 GHz	14 kHz ~ 1 GHz	100 kHz ~ 30 MHz

Radiated emission from the IES and interference with the X-band receiver

The anechoic chamber and the measurement room at ISAS are shown schematically in the Figure 1. This facility has radio wave absorbers attached to all wall surfaces, as well as the ceiling and the floor, with electromagnetic shields. This chamber is used for antenna pattern measurements, EMC tests between observation equipments and telemeters or radar transponders of either scientific satellites or rockets, and for tests involving observation equipment with wireless transmission functions. In the RE02 measurement and XRX interference test, a PM of the IES thruster control unit (ITCU), a PM of microwave oscillator and a flight model (FM) of a traveling wave tube amplifier (TWTA), a PM of μ10 ion source and a PM of neutralizer were used. However, a PM of an IPPU which was not available due to its tight schedule and propellant feed system which seemed to have clearly no relation to EMI were replaced with ground

support equipments (GSE) comprising a mass flow controller and commercial high voltage DC power supplies.

Radiated emission from the IES can be divided into two categories: 1) Emission having its origin at the IPPU, such as switching noise or ripples; 2) Noise emanating from the plasma acting as a "load", which appears when the IPPU is operated in combination with the ion source and the neutralizer. The former can be easily reproduced and tackled through tests using resistive loads simulating ion thruster heads. There was no difference in conducted noise emission on the screen- and decel- grid lines between the case using a GSE and the case using an IPPU, except apparent switching noises of IPPU at the switching frequency and its harmonics. Therefore, if we concentrate on the noise originated from the plasma, the RE measurement result in the GSE operation can be considered same as the measurement result of IES with EMI optimized flight model (FM) of the IPPU.

It is difficult to measure electromagnetic emission from the ion engine system due to the metallic tank for the usual operation on the ground. Also, a glass chamber consisting of a cryopump, a cylindrical glass wall and an IES-mounting metal flange was prepared. An ion thruster and a neutralizer were hang from the top flange, and the chamber was evacuated using the cryopump. The IES was operated at Xe flow rates of 1.85 SCCM for the main discharge and 0.4 SCCM for the neutralizer, which correspond to 80 % of the nominal thrust level, due to the limited exhaust capability of the cryopump. With this less flow rate, the higher background pressure in the glass chamber increased the ion beam current to over 130 mA which corresponds to the nominal thrust level of 7 mN.

Radiated emission from the neutralizer

The experimental setup to measure radiated emissions from the neutralizer is shown in Figure 2. The electromagnetic shield characteristics of the EMI chamber at ISAS is better than the anechoic chamber described before, and EMI measurements of small onboard equipments are usually conducted in this room. Because the cylinder glass chamber was too large to be carried in the EMI chamber, it was not possible to carry out the IES radiation noise measurement here. A 30-mm-square punching steel plate, acting effectively as an anode, was placed 20-mm downstream from the neutralizer. As a microwave supply system, a GSE which consisted of an oscillator and a solid-state amplifier was used. The neutralizer was installed in the small T-shaped glass chamber, evacuated with an oil diffusion pump, and an electron current equivalent to the one of nominal IES operation was extracted.

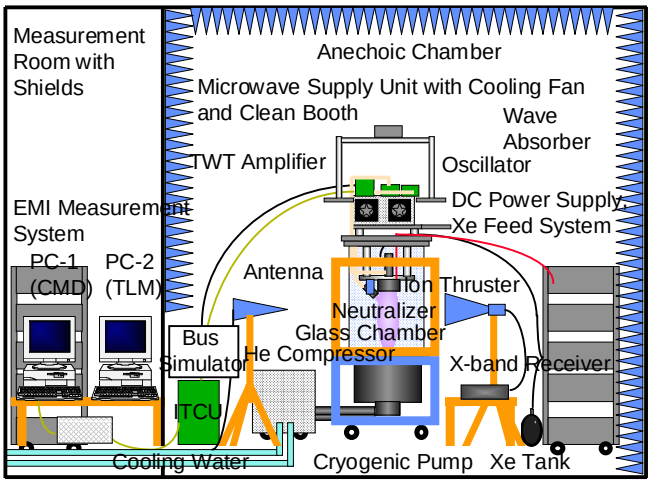

Figure 1 - Experimental setup to measure radiated emissions from MUSES-C/IES and to check the interference with the X-band receiver.

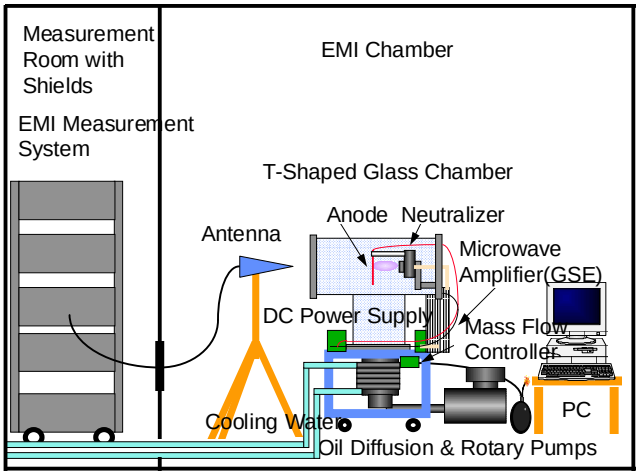

Figure 2 - Experimental setup to measure radiated emissions from the neutralizer.

Conducted emission from the IES

This measurement was performed in a room equipped ion engine endurance testing capabilities, which was not shielded from external electromagnetic noise. The measurement of the conducted noise can be simply carried out only by installing current probes for the

wirings, and the effect of the external noise was not observed whatsoever. Though the wirings used were common vinyl lines and were not flight-qualified, this had no effect on the measurement results, even if they were replaced by well-shielded coaxial cables. Accordingly, the cable type was considered to be independent in the properties of the conducted noise. The measurement was carried out at 3 points: screen current line, neutralizer current line, and hot line of the spacecraft bus simulator. Because the PM of the IPPU had not been well tuned considering the EMI characteristics yet and had its own switching noise independent of the load characteristics, the measurement with the IES operating with a GSE in order to distinguish plasma-oriented noise, was also carried out.

Experimental results and discussion

RE02 background noise

Concerning radiated emission measurements, in accordance to RE02 specification of MIL-STD-461C, background noise was observed at the onset of the experiment, when the ITCU and GSE including a computer, vacuum pumps, and DC power supplies were all kept switched on but not in operating condition. This noise factor was subtracted from the data from the overall IES case as well as for the case of the neutralizer operating independently. Both narrowband (NB) and broadband (BB) E-field emissions were measured simultaneously, but only the former data are reported in this paper. The units for the vertical axis of the graphs of the RE02 results are given in dBμV/m. Figure 3a shows much more noise in the anechoic chamber than in the EMI chamber at frequencies less than 1 GHz, due to the superior electromagnetic shield capability of the EMI chamber. In the anechoic chamber, the external noise was more remarkable than the noise generated by the equipments inside. In both facilities there were a lot of frequency bands in which background noise deviated the restriction of MIL-STD shown by the polygonal line in Figure 3a and are not ideal for noise measurement. However, good shielding characteristics were shown for frequencies over UHF, often used for telecommunications, and in those no noise exceeded the internal noise of measuring instruments over 1 GHz. Only the result of the anechoic chamber is shown in Figure 3b. The straight line which shows monotonous increase in Figure 3b provides the MIL-STD-461C specification, and the two added notches indicate an uplink frequency of 7.16 GHz for MUSES-C's XRX and its image frequency of 6.36 GHz.

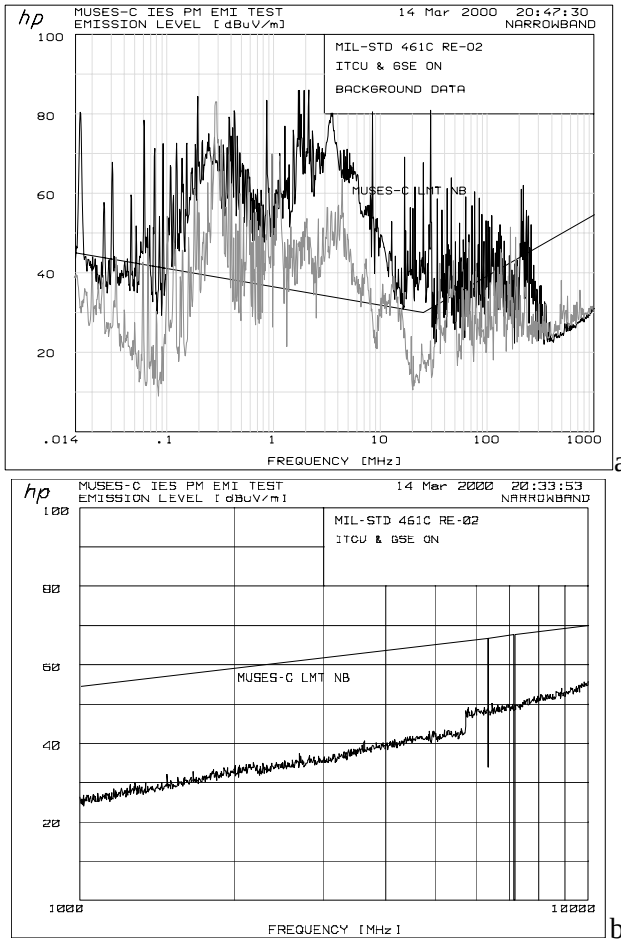

Figure 3 - RE02 Background noise and EMI specification of MUSES-C spacecraft.

a) 14 kHz ~ 1 GHz
upper: in the anechoic chamber.
lower: in the EMI chamber.

b) 1 GHz ~ 10 GHz in the anechoic chamber.

RE02 14 kHz ~ 1 GHz

Low-frequency noise spectrums under 1 GHz during the IES operation are shown in Figure 4. Here, although the background noise is already deducted from the measured data, in the frequency band where background noise is originally large, such noise can not be totally removed. Figure 4a shows noise emission in the condition of plasma discharge of both the ion source and the neutralizer. There was no noise larger than the background noise and it means that radiation from the IES in discharge mode is negligible. Once the high voltage DC power supply was turned on and the ion

beam acceleration was started, a broadband noise with a tendency for the intensity to increase at lower frequencies, and which is apparently larger than background noise as shown in Figure 4b, was generated. This deviates from the restriction by 30 ~ 40 dB at frequencies under 5 MHz. Even though there are a number of sharp upsurges and drops in the 2 ~ 4 MHz frequency range, it is not clear whether this is due to the IES operation since the background noise reaches its maximum level around this frequencies and its random fluctuation may influence the result.

Figure 5 shows the results of the neutralizer operations in the EMI chamber. This set of data has comparatively smaller effects of the background noise. It is not clear why the emission by the neutralizer discharge by itself, as shown in Figure 5a, is at maximum 20 dB larger than the emission by both main and neutralizer discharges as shown in Figure 4a. Figure 5b shows the noise when the electron current is extracted to the anode from the neutralizer at a bias voltage about 30 V. This noise spectrum resembles the spectrum emitted by the IES during the beam acceleration as shown in Figure 4b, indicating that most of the low-frequency noise under 5 MHz is originated from the neutralizer plasma. Similar results for neutralizer noise have also been reported for the T5 ion thruster [6] in combination with a Kaufman-type ion source and a hollow cathode neutralizer. It will be added that both devices adopted a plasma production mechanism completely different from the one in the MUSES-C/IES'.

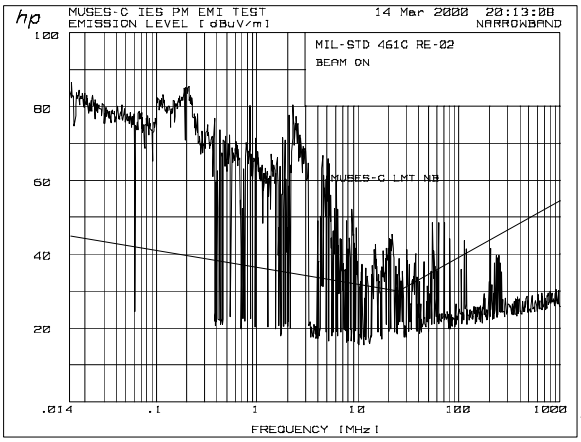

b)

Figure 4 - RE02 Narrow band noise from the ion engine system.
14 kHz ~ 1 GHz (with background noise subtracted)
a) The neutralizer and main discharge.
b) The thruster at 7 mN.

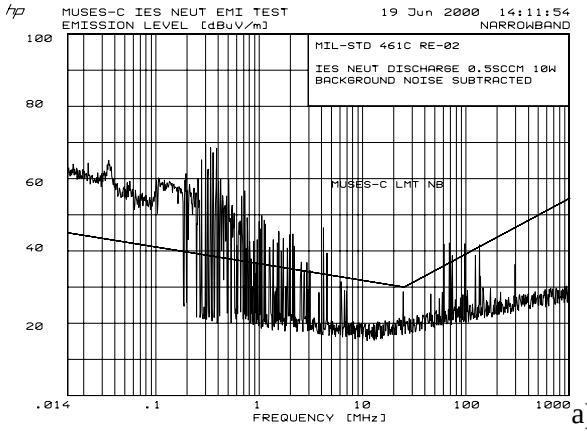

a)

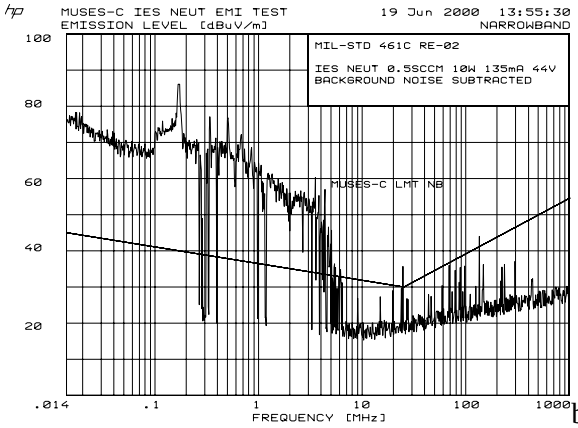

b)

Figure 5 - RE02 narrowband noise from the neutralizer.
14 kHz ~ 1 GHz (with background noise subtracted)
a) Neutralizer discharge.
b) Electrons are extracted.

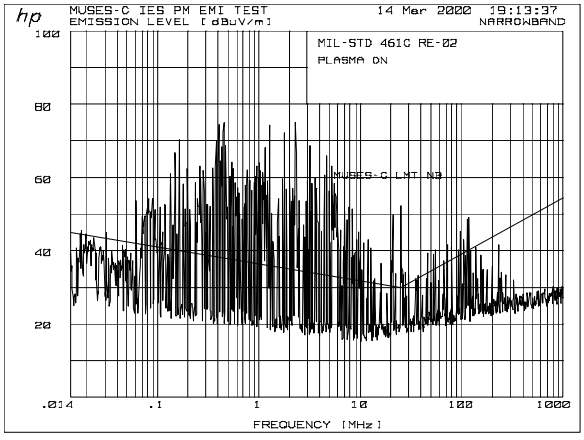

a)

CE-02 100 kHz ~ 30 MHz for power line and noise in screen and neutralizer current lines

The low-frequency radiated emission below 5 MHz suggests that conducted noise, which has a similar spectrum, influences other equipments on the spacecraft by propagating through four feeding lines including screen, accelerator, neutralizer, and return lines from the IPPU to the thruster heads, by way of the unstabilized spacecraft power line to which the three IPPUs are connected. Incidentally, not only the usual CE-02 measurement on the power line but also measurement of the spectrum of alternating current components, which are included in the current-to-screen grid and from neutralizer, were carried out. The neutralizer and the decelerator grid were wired at the same potential in such IES.

Figures 6 ~ 8 show the spectrum of the conducted noise on screen- and neutralizer-current in the case of using the GSE of DC power supplies instead of an IPPU. The units in the vertical axis of the graphs for the CE02 results are given in dBm, and its reference (0 dBm) corresponds to a current amplitude of 447 mA in this measurement, with the current probe gain and the spectrum analyzer's input impedance. Note that a -20 dB difference in this figure indicates an amplitude decrease by one order of magnitude. Figure 6 and Figure 7 show the change of low-frequency noises under 300 kHz which were measured in the screen current line and the neutralizer current line in plasma discharge mode and in beam acceleration mode. It is proven that the noise of the neutralizer current is very larger than that of the screen current in beam acceleration mode, though the noises in plasma discharge mode are small for both. This fact is so easy to notice just in monitoring neutralizer current history with a multi-channel digital recorder that a 5-Hz filter function should be enabled to eliminate the noise whose amplitude reaches 70% of the neutralizer current. On the neutralizer line, coherent oscillations which have a fundamental frequency of 160 kHz and its harmonics up to the fifth.

Condition of the oscillation generation and the characteristic frequency are dependent on xenon flow rates and neutralizer currents. The oscillation was not observed only in the conducted noise on the neutralizer line shown in Figure 7 but also radiated emission spectrum measured by operating the neutralizer by itself as shown in Figure 5b. Although the narrowband noise peak found in the radiated emission from the IES shown in Figure 4b has a slightly higher frequency of about 200 kHz, it may be regarded as fundamentally the same phenomenon. The oscillation reappeared in the same fashion with additional switching noise from the IPPU other frequencies when an IPPU instead of GSEs was used, and it was also the same case when the operation of only the neutralizer was performed. This implies that the neutralization processes in the ion beam and the power supply characteristics are unrelated to both the oscillation and the low-frequency noise. Results concerning a more detailed investigation of the correlation between neutralizer operating conditions and the oscillation, as well as its generation mechanism, will be reported later in this paper.

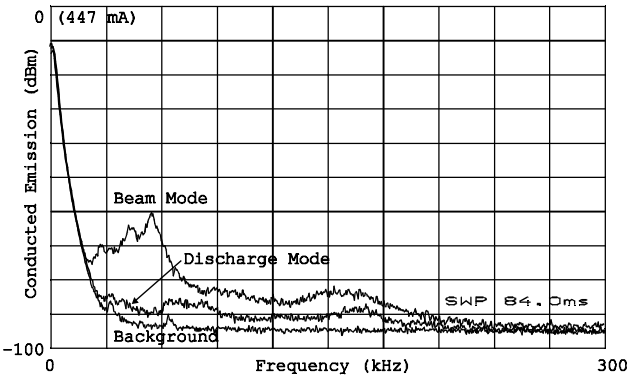

Figure 6 - CE measurement result for screen grid line over the frequency range 0 to 300 kHz.

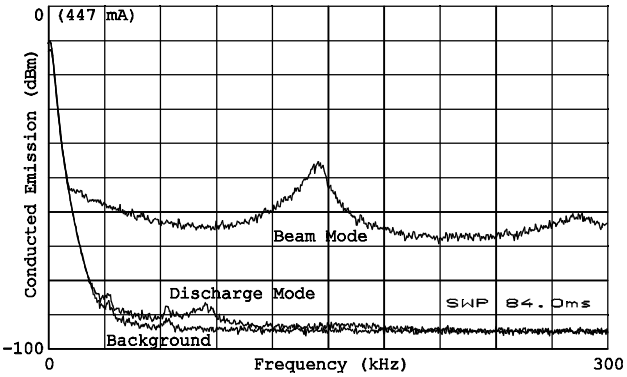

Figure 7 - CE measurement result for neutralizer line over the frequency range 0 to 300 kHz.

The noise tails of the screen current and neutralizer at high frequencies up to 5 MHz are both shown in Figure 8. As for neutralizer there is almost no noise over 4 MHz. Figure 8 shows that the screen current contains small amount of noise in the 500 kHz ~ 4 MHz frequency range. Incidentally, this finding cannot be estimated just by inspecting Figure 6, which shows the

decrease at relatively higher frequencies right below 300 kHz.

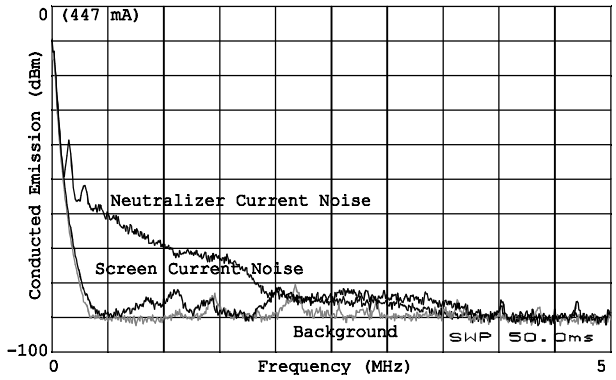

Figure 8 - CE measurement results for screen grid line and neutralizer line over the frequency range 0 to 5 MHz.

Though there was conducted noise correlative with radiated noise in the wires connected with the ion thruster head, noise caused by the engine could not be observed in the results concerning CE02 measurements of the simulated spacecraft power line to the IPPU, as shown in the lower data of Figure 9. The upper trace of Figure 9 shows the result when operating the IPPU connected to resistors as dummy loads replacing the thruster head. However, significant differences in both results even in the low frequency region where the RE and CE appear were not found. This is probably because most of the power consumption by the IPPU is made by the beam current with much less noise, and the noise power of the neutralizer is too small to influence the bus power. By raising the frequency resolution of the spectrum analyzer, it turned out that the power line current noise consists of switching noise of the IPPU at frequencies of 100 kHz and its very high order harmonic components. However, at present, irrespective of whether a resistive or plasma load is considered, the noise level exceeds the MUSES-C specification limits, which require emissions lower than 40 dBμA below 3 MHz, and lower than approximately 20 dBμA for the 5 ~ 17 MHz frequency range. It was judged that elimination of the switching noise leak will be easy when manufacturing the FM of the IPPU, since circuit design and mounting considering the EMI characteristics had not been completely carried out in the PM of the IPPU. Besides, the MUSES-C specification was too strict by 20 dB in comparison with MIL-STD, which was just satisfied by the PM IPPU, and can be relaxed to the same level. Since the test clarified the fact that the noise from IES plasma does not affect the spacecraft power bus, the EMC tuning of the flight model is possible with the IPPU by itself without fitting to other IES components.

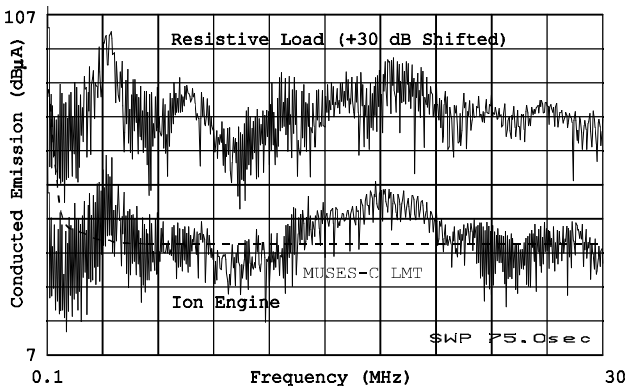

Figure 9 - CE02 measurement result for IPPU's power line over the frequency range 100 kHz to 30 MHz, compared with the result in resistive load operation.

More details on the low-frequency neutralizer noise

In order to understand the characteristics of the noise emission from the neutralizer at low frequencies, further parametric studies were carried out. Figure 10 shows two typical time histories of the neutralizer current recorded with a digital memory recorder at a relatively slow sampling time of 50 μs. At a xenon flow rate of 0.5 SCCM there was noise with an amplitude as large as the 140 mA direct current component, as shown in Figure 10a. Nonetheless, it decreased in overall amplitude to 1/3 of the noise level shown in the upper trace, at an excessive flow rate of 1.0 SCCM as shown in Figure 10b.

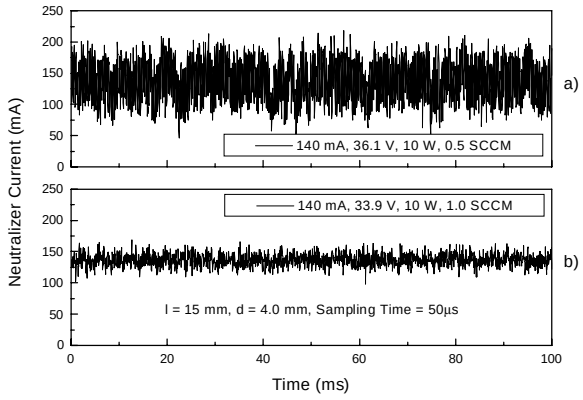

Figure 10 - Time domain waveforms of the neutralizer current.
a) Noise in nominal operation.
b) Less noise at a larger mass flow rate.

Frequency spectra of conducted neutralizer noise are shown in Figure 11 for several operating conditions. Nomenclatures used are as follows.

V_D : Voltage between the neutralizer and the anode.
I_D : Electron emission current.
P_μ : Microwave power for plasma discharge.
$\dot{m}$: Xenon flow rate.
l: Anode distance from the neutralizer
d: Neutralizer orifice diameter

Broadband noise below 5 MHz and narrowband noise by coherent self oscillation with harmonics can be seen. In the case with just a plasma discharge without electron extraction taking place, conducted emission was not observed, as shown in Figure 11a. After increasing the electron current to about 15 mA, broadband noise and the noise level saturated at the current of 70 mA were generated. Comparing Figure 11b and Figure 11c, it is seen that increasing xenon flow produces a decrease in broadband noise and suppresses the oscillation. Comparison of Figure 11b and Figure 11d suggests that it is impossible to suppress the coherent oscillation, although the broadband noise can be reduced by decreasing the microwave power.

Next, a scaling of the fundamental frequency of the coherent wave, ranging over 150 ~ 200 kHz was investigated by changing parameters such as $\dot{m}$, d and l. Table 2 summarizes the frequency of appearance of such oscillations when d and l are changed, and shows that when the ratio of d to l is large, the oscillation is infrequent. We may consider d as a characteristic length describing the diameter of the plasma column blowing out of the neutralizer, and l as a characteristic length describing the plasma column length. Strictly speaking, a plasma column has diameter distribution in axial direction, and increasing l may also increase the column diameter. In that sense l and d are not perfectly independent parameters.

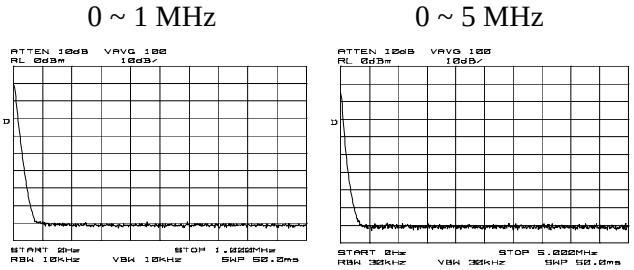

a) V_D = 0 V, I_D = 0 mA, P_μ = 10 W, $\dot{m}$ = 0.5 SCCM.

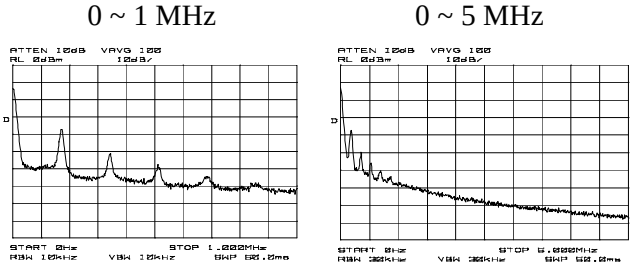

b) V_D = 42.0 V, I_D = 140 mA, P_μ = 10 W, $\dot{m}$ = 0.5 SCCM.

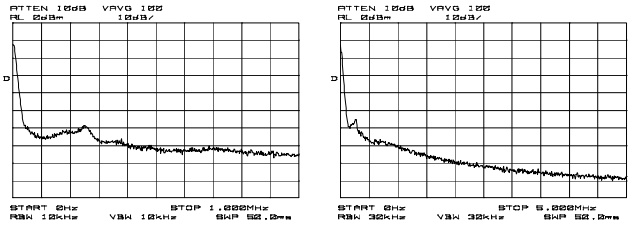

c) V_D = 33.0 V, I_D = 140 mA, P_μ = 10 W, $\dot{m}$ = 1.0 SCCM.

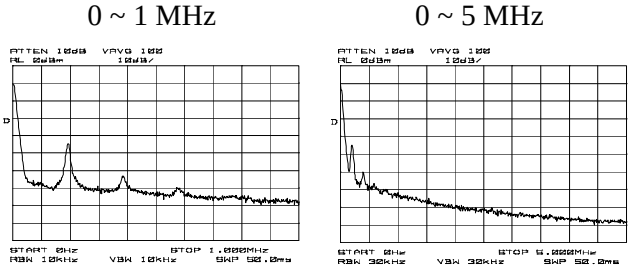

d) V_D = 62.1 V, I_D = 140 mA, P_μ = 5 W, $\dot{m}$ = 0.5 SCCM.

Figure 11 - Noise spectra of neutralizer current.
l = 20 mm, d = 4.5 mm, 10 dB/div.

Table 2. Coherent oscillation occurrence probability and parameters relating to the shape of plasma plume.

d (mm) / *l* (mm)	10	15	20	30
4.0	⛆	☒	☒	☒
4.5	☑	☒	☒	☒
5.0	-	⛆	☒	☒
5.5	-	-	☑	☒
6.0	-	-	-	⛆

☒: Oscillation observed at various currents and flow rates.
⛆: Oscillation observed at some currents and flow rates.
☑: Oscillation never occurred.
- : Not tested.

Although strong oscillations clearly provide a sharp peak, a weak oscillation tends to have a broad spectrum and its representative frequency is not obvious. This is the cause of the ambiguity of the peak frequency and is expressed in terms of error bars in the figures below. Figure 12 shows typical variations of oscillation intensities and fundamental frequencies as functions of xenon flow rates. The intensity usually has a peak at certain flow rate and decreases at larger flow rates, as shown in Figure 12a. Figure 12b illustrates a weak dependence of the frequency on the flow rate and is inclined to decrease as the flow rate increases.

Figure 13 provides the fundamental frequency variations with respect to neutralizer current. The neutralizer current was swept from 100 to 300 mA with an orifice diameter and xenon flow rate fixed at 4.5 mm and 0.5 SCCM, respectively. The frequency always increases by increasing the current. Four anode distances *l* were chosen as a parameter, and it is shown that the larger the value of *l* is, the lower the value of the frequency, even though such dependency is rather weak.

Figure 14 shows the frequency change as a function of the orifice diameter *d*. The frequency is smaller when *d* is larger. In spite of the change of *d* from 4.0 to 6.0 by a factor of 1.5, the factor by which the accompanied changes lies between 1.3^{-1} and 1.1^{-1}, which can be interpreted as a nearly inversely proportional relation between *f* and *d*. With fixed flow rate, a 1.5 times larger orifice makes the neutral pressure in the neutralizer discharge chamber 2.25 times higher. Because the relationship between the flow rate and the frequency *f* has a negative slope, as given in Figure 12, if the pressure is maintained constant, *f* and *d* will show a more evident inversely proportional relation.

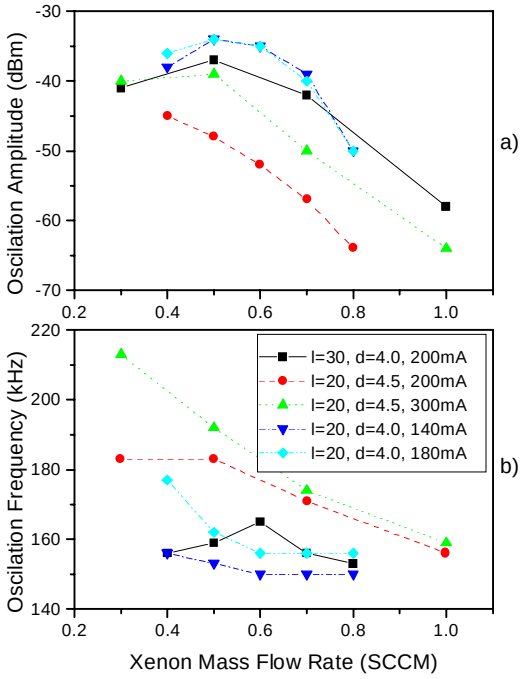

Figure 12 - Typical variation of oscillation intensities and fundamental frequencies as functions of xenon flow rates. P_μ = 10 W.

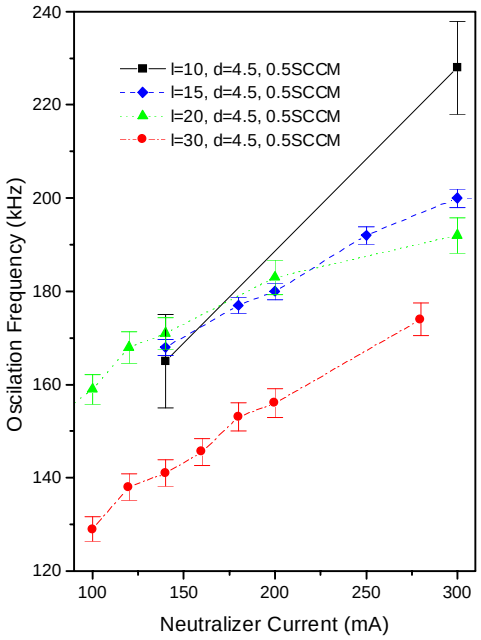

Figure 13 - Fundamental frequency versus neutralizer current curves weakly dependent on the anode distances *l*. d = 4.5 mm, $\dot{m}$ = 0.5 SCCM, P_μ = 10 W.

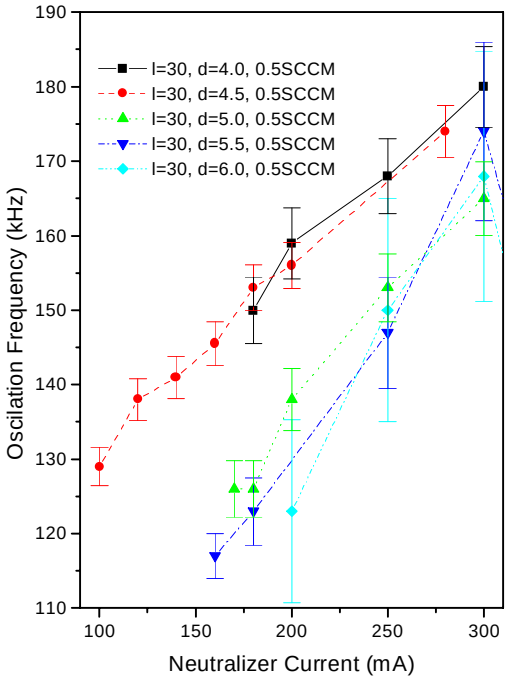

Figure 14 - Fundamental frequency versus neutralizer current curves dependent on the orifice diameters d. l = 30 mm, $\dot{m}$ = 0.5 SCCM, P_μ = 10 W.

What is the cause of the coherent noise in the microwave discharge neutralizer at 160 kHz? When a current is applied to plasma, oscillations at frequencies lower than the ion plasma frequency are often observed. Such phenomenon is generally known as current-driven ion acoustic instability. There are reports that in most case it is an oscillation in axial direction along with the electron current, whose wavelength is twice the plasma column length and whose phase velocity equals the ion sound velocity or the ion thermal velocity [10],[11],[12]. Although there are several interpretations for the oscillation mechanism, it is generally thought that the reciprocal of the ion transit time τ_i, calculated by using the ion thermal velocity and the plasma column length l:

$$1/\tau_i = \sqrt{3kT_i/m_p}/l$$

basically represents the oscillation frequency, where k is the Boltzmann constant, m_p is the ion mass and T_i is the ion temperature. Assuming T_i = 0.04 eV, a value of 14 kHz is obtained. However, this value is much smaller than the experimentally observed value of 160 kHz, and certainly too small to explain the oscillation by an longitudinal oscillation mode.

Nevertheless, there is a report by Crawford [13] in which the radial mode of an ion acoustic wave is most probable. He conducted experiments by using several kinds of direct current discharge plasmas with hot cathodes and various diameter glass tubes, and found low frequency oscillations below 1 MHz, exactly as in our results. According to this publication, the fundamental frequency f is given by

$$f = (2.405/\pi d)(\gamma kT_e/m_p)^{1/2}$$

where d is the diameter, γ is the specific heat ratio (= from 1 to 3) and T_e is the electron temperature. The constant 2.405 is the minimum number which makes the Bessel function zero. Assuming T_e = 3.5 eV and f = 160 kHz, we obtain d = 7.7 (γ = 1) ~ 13.2 (γ = 3) mm, which is comparable to the real orifice size or slightly larger. This and the experimentally obtained relation, fd = const., suggests that the radial mode of standing ion acoustic wave exists in the plasma column in front of the microwave discharge neutralizer.

RE02 1-10 GHz and X band receiver interference test results

Microwave leakage at frequencies of 4.25 GHz and 8.5 GHz were detected when microwave dummy loads replaced the ion source and the neutralizer in the anechoic chamber. Still, their levels were below the MUSES-C limit by 10 dB and we did not specify the leakage position. The radiated emissions in the discharge mode and beam acceleration mode were too strong to measure with the nominal setup of the measuring instruments. As shown in Figure 15 the obtained data is saturated at the two frequencies. The 4.25 GHz peak has a spread which is originated from the spurious characteristics of the TWTA and not from non-linear phenomena of the discharge plasma. These emissions at two frequencies are caused by leakage of the supplied microwave power through the grid holes of the ion beam optics and the neutralizer orifice.

The radiated emissions measured again without the pre-amplifier normally used, with a 20 dB attenuator, are summarized in Table 3. The microwave leakage was 10 dB larger in the beam acceleration than in the plasma discharge at the electron cyclotron resonance frequency of 4.25 GHz. It is shown that the leakage increases as the plasma density is lower. As for the emission at the second harmonic frequency of 8.5 GHz, the leakage is independent of the plasma density, and it is indicated

that there is originally no absorption by the plasma at that frequency. In this experiment using the cylindrical glass chamber, the thrust level was throttled to 80 %, but it turned out to be a more severe testing condition from the viewpoint of microwave noise emission, in which the plasma density was lower and noise leakage increased. If we assume that the leaked electromagnetic wave from the IES is a spherical wave, the leaked powers can be calculated as 66 mW at 4.25 GHz and 1.9 mW at 8.50 GHz. For effective utilization of supplied microwave power of about 40 W for plasma generation in an ion source and a neutralizer, these losses are sufficiently small and not problematic.

In order to provide a reference to reflect the radiated susceptibility (RS) specification of MUSES-C, E-field intensities at a distance of 1 m were calculated as shown in Table 3, given in V/m units. In the original MUSES-C specification the required level had been determined as 5 V/m for high frequencies over 30 MHz. As an illustrative example, assuming the worst case in which a equipment is located at a distance of 0.3 m from thruster heads and three ion engines are operated simultaneously, the E-field intensity at that position would be calculated as

$$3.3 \times \sqrt{(1.0/0.3)^2} \times \sqrt{3} = 19\,\mathrm{V/m}\,.$$

Thus the RS specification at 4.2 GHz was modified to 20 V/m and the RE specification was waived for the IES. The philosophy of the RS specification at the RF frequency for plasma production of microwave discharge ion thrusters may be identical with other transmitters onboard spacecraft.

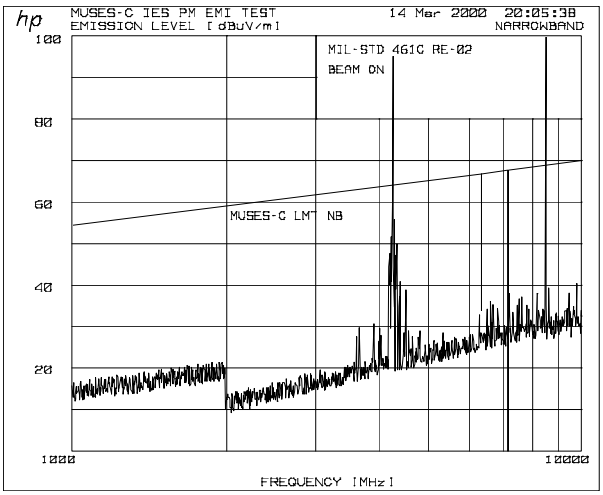

Figure 15 - RE02 Narrow band noise from the ion engine system at 7 mN.
1 - 10 GHz (with background noise subtracted)

Table 3. Microwave leakages at a distance of 1 m at oscillator frequency, its second harmonic and X-band uplink frequency of MUSES-C spacecraft.

	4.25 GHz	8.5 GHz	7.16 GHz
Operating at 7 mN	130.4 dBμV/m (3.3 V/m)	99.7 dBμV/m (0.097 V/m)	-48.72 dBμV/m
Main and neutralizer discharge	119 dBμV/m (0.89 V/m)	99.2 dBμV/m (0.091 V/m)	-48.82 dBμV/m

The power density at the 7.16 GHz X-band uplink frequency was calculated from the results of the interference test with the PM of the XRX. Table 4 shows the change of the noise level detected by the XRX depending on the operating condition of the IES. Because a larger amount of noise was observed when there was no plasma or its density was smaller, it is thought that very weak spurious signals originating at the microwave amplifier leaked from the ion source as well as from the neutralizer at 7.16 GHz. The low gain antenna C (LGA-C) of the MUSES-C spacecraft, which is located most closely to the IES and is easily affected by radiated emissions, is designed to output an estimated noise power of -210.2 dBm/Hz considering the distance, the angle separation and the antenna gain pattern. This is sufficiently small compared to the internal noise level (-173 dBm/Hz) of the receiving system, and so it is concluded that no adverse effect is given to the XRX, even in the case when the three ion engines are operating at the same time with the maximal thrust levels.

Table 4. Noise levels observed with the X-band receiver at several IES conditions.

Ion source	Neutralizer	Noise level
Beam extraction	Electron extraction	0.6 dB
Discharge	Discharge	0.5 dB
Discharge	Microwave introduction without Xe gas	0.7 dB
Microwave introduction without Xe gas	Microwave introduction without Xe gas	1.1 dB
No operation	No operation	0 dB (Background noise floor)

Conclusions

Comparing the results of EMI measurements using the IES of the MUSES-C asteroid sample return mission and the neutralizer operating independently, it was found that radiated emissions from the IES exceeding the MIL-STD-461C originate mainly from the neutralizer. Radiated emission in the high frequency range above 1 GHz was not observed, except at the oscillator frequency and the second harmonic frequency of the TWTA utilized for plasma production, which leaks from the exit of both the ion source and the neutralizer. It is concluded that the operation of the IES does not interfere with the XRX of the MUSES-C, based on the findings of the test using the PM of the XRX. Although the IES needs no longer satisfy RE specification, the final check for electromagnetic compatibility between the IES and the spacecraft, not only in steady-state operation but also in transient phenomena, such as high voltage breakdown between grids, will be carried out by the operating an ion engine in the glass chamber located in the vicinity of the flight model of the MUSES-C spacecraft.

Acknowledgments

The authors wish to thank Professor Z. Yamamoto and Mr. Y. Kamata of ISAS, Mr. F. Fuke of NEC and the rest of the MUSES-C communication subsystem staff for their cooperation concerning this series of tests.

[1] J.S. Sovey, L.M. Carney, S.C. Knowles, "Electromagnetic Emission Experiences Using Electric Propulsion Systems," *Journal of Propulsion and Power* ***5****, 534 - 547*, 1989.

[2] Y. Nakamura, and S. Kitamura, "Research on 5 cm Diameter Mercury Ion Thruster," *Acta Astronautica* ***7****, 1075 - 1089*, 1980.

[3] I. Kudo, K. Machida, Y. Toda and H. Murakami, "Electromagnetic Noise from an Ion Engine System," *J. Spacecraft and Rockets* ***20***, 84-88, 1983.

[4] S. Shimada, H. Takegahara, Y. Gotoh, K. Satoh, and K. Kajiwara, "Ion Engine System Development of ETS-VI," *AIAA Paper 89-2267*, 1989.

[5] H. Muller, R. Kukies and H. Bassner, "EMC Tests on the RITA Ion Propulsion Assembly for the ARTEMIS Satellite," *AIAA Paper 92-3208*, 1992.

[6] S. Chanda, F. Mawdsley, R.D. Brown, S.D. Watson, A.K. Malik and D.G. Fearn, "Measurements of the Electromagnetic Emissions from the T5 Ion Thruster," *IEPC Paper 93-234*, 1993.

[7] J. Wang, D.E. Brinza, D.T. Young, J.E. Nordholt, J.E. Polk, M.D. Henry, R. Goldstein, J.J. Hanley, D.J. Lawrence and M. Shappirio, "Deep Space One Investigations of Ion Propulsion Plasma Environment," *J. Spacecraft and Rockets* ***37***, 545 - 555, 2000.

[8] K. Toki, K. Kuninaka, I. Funaki, K. Nishiyama, and Y. Shimizu, "Development of a Microwave Ion Engine System EM for MUSES-C Mission," *22nd International Symposium on Space Technology and Science*, 2000-b-09, 2000.

[9] N. Onodera, H. Takegahara, I. Funaki, and H. Kuninaka, "Interaction between Plasma Plume of Electric Propulsion and Spacecraft Communication," *IEPC Paper 99-228*, 1999.

[10] I. Alexeff, and R.V. Neidigh, "Observations of Ionic Sound Waves in Plasmas Their Properties and Applications, " *Phys. Rev.* ***129***, 516-527, 1963.

[11] A. Barkan, N. D'Angelo, and R.L. Merlino, "Potential Relaxation Instability and Ion Acoustic Waves in a Single-ended Q-machine Dusty Plasma," *Physics Letters [Part A]* ***222***, 329-332, 1996.

[12] C.A. Capeau, G. Bachet, and F. Doveil, "Plasma Self-oscillations in the Temperature-Limited Current Regime of a Hot Cathode Discharge," *Phys. Plasmas* ***2***, 4650-4655, 1995.

[13] F.W. Crawford, "Electrostatic Sound Wave Modes in a Plasma," *Physical Review Letters* ***6***, 663-665, 1961.